

Magnetic-Field-Switchable Laser via Optical Pumping of Rubrene

Collin F. Perkinson, Markus Einzinger, Joseph Finley, Mounji G. Bawendi, and Marc A. Baldo*

Volumetric optical imaging of magnetic fields is challenging with existing magneto-optical materials, motivating the search for dyes with strong magnetic field interactions, distinct emission spectra, and an ability to withstand high photon flux and incorporation within samples. Here, the magnetic field effect on singlet-exciton fission is exploited to demonstrate spatial imaging of magnetic fields in a thin film of rubrene. Doping rubrene with the high-quantum yield dye dibenzotetraphenylperiflanthene (DBP) is shown to enable optically pumped, slab waveguide lasing. This laser is magnetic-field-switchable: when operated just below the lasing threshold, application of a 0.4 T magnetic field switches the device between nonlasing and lasing modes, accompanied by an intensity modulation of +360%. This is thought to be the first demonstration of a magnetically switchable laser, as well as the largest magnetically induced change in emission brightness in a singlet-fission material to date. These results demonstrate that singlet-fission materials are promising materials for magnetic sensing applications and could inspire a new class of magneto-optical modulators.

crystalline materials, garnets, or rare earth-doped paramagnetic glasses and are thus poorly suited to large-area and volumetric imaging.^[4] Nitrogen vacancy (NV) centers provide high sensitivity to magnetic fields (on the order of 1 nT Hz^{-1/2} for a single NV center),^[5] but NVs suffer from weak optical cross section, a requirement for high resolution detection of their emission wavelength, and difficult calibration.^[6] Magnetic imaging applications would benefit from stronger optomagnetic interactions within biocompatible materials such as molecules or nanoparticles, which could be directly incorporated within a sample or bioassay.^[7] Nanomaterials for magnetic imaging are ideally also capable of high-resolution imaging and operation at high photon flux, potentially even in microlasers, where brilliant emission and high spectral sensitivity creates new opportunities to monitor a wide

1. Introduction


The difficulty of optically imaging magnetic fields poses a challenge for many technologies. Optical interrogation of magnetic fields could be used to study spintronic materials that lack inherently strong Kerr effects,^[1] improve the resolution of magnetic resonance images (MRI),^[2] and locate magnetic nanoparticles in biological assays.^[3] Traditional approaches to magnetic field imaging that exploit weak magneto-optical interactions such as the Faraday effect are typically reliant on expensive

range of physiological parameters with cellular resolution.^[8] New optomagnetic effects in fluorescent or electroluminescent materials could be used to modulate lasers and may even find new applications in optical modulators, which presently rely on weak thermal or electro-optic effects.

One alternative to conventional magneto-optical materials is suggested by proposed explanations for the sensitivity of birds to Earth's magnetic field. Recent studies suggest that birds are able to orient themselves to Earth's magnetic field by exploiting the magnetic sensitivity of electronic interactions in their retinas.^[9,10] Photoexcitation of proteins in avian retinas produce radical (unpaired electron) intermediate states, which then interact with spin-1 excitons (electron-hole pairs), also known as triplet excitons. To understand the basis for the magnetic dependence of these interactions, consider an asymmetric molecule, for which the three triplet states of the spin-1 exciton are energetically split even in the absence of a magnetic field. Typically, without substantial spin-orbit coupling, this zero-field splitting is less than about 10 μeV .^[11] Therefore, an external magnetic field on the order of 10 $\mu\text{eV } \mu_B^{-1}$ (≈ 0.2 T), where μ_B is the Bohr magneton, can reorder the triplet states via the Zeeman effect, modulating their involvement in spin-dependent interactions. The magnetic field sensitivity is typically even higher for an unpaired electron with no zero-field splitting. Consequently, both triplet-triplet and triplet-charge interactions can undergo magnetic field modulation. Given its

C. F. Perkinson, M. G. Bawendi
 Department of Chemistry
 Massachusetts Institute of Technology
 77 Massachusetts Avenue, Cambridge, MA 02139, USA

M. Einzinger, J. Finley, M. A. Baldo
 Department of Electrical Engineering and Computer Science
 Massachusetts Institute of Technology
 77 Massachusetts Avenue, Cambridge, MA 02139, USA
 E-mail: baldo@mit.edu

 The ORCID identification number(s) for the author(s) of this article can be found under <https://doi.org/10.1002/adma.202103870>.

© 2021 The Authors. Advanced Materials published by Wiley-VCH GmbH. This is an open access article under the terms of the Creative Commons Attribution License, which permits use, distribution and reproduction in any medium, provided the original work is properly cited.

DOI: 10.1002/adma.202103870

effectiveness in avian magnetoreception, exploiting the magnetic field dependence of spin interactions in small organic molecules and nanoparticles may provide a compelling alternative to conventional magneto-optical materials for magnetic sensing.

Rubrene is a well-studied organic molecule that exhibits a strong magnetic field effect due to the magnetic field dependence of singlet fission (SF). During SF, a spin-singlet exciton splits into a pair of spin-triplet excitons with overall spin-singlet character. Some of these triplet–triplet pairs undergo diffusive separation and nonradiative recombination, while others recombine into a singlet exciton via the reverse process of SF known as triplet–triplet annihilation (TTA), or triplet upconversion. Triplet upconversion, and in turn SF, is affected by the presence of a magnetic field, which modulates the coupling between the triplet–triplet pair states and the singlet state.^[12,13] The change in coupling between triplet–triplet pair states and the singlet state is responsible for the increase in photoluminescence under magnetic field of rubrene.

In this work, we exploit the magnetic field dependence of singlet fission in rubrene to demonstrate strong magneto-optical interactions and spatial imaging of magnetic fields. Furthermore, we show operation under high optical flux in a magnetic-field-switchable laser. This laser, achieved via optical pumping of a rubrene slab waveguide doped with the high-quantum-yield dye dibenzotetraphenylperiflanthene (DBP), is shown to exhibit an $\approx 7.2\%$ reduction in lasing threshold in the presence of a ≈ 0.4 T magnetic field. The laser undergoes both spectral and spatial narrowing as a function of optical pump power, and it exhibits multimode lasing, which can be turned on and off by an applied magnetic field. The device achieves a peak magnetic modulation in output intensity of +360% when pumped just below the lasing threshold. This represents a new class of optical modulation that can be switched between “on” and “off” states as a function of applied magnetic field. To the best of our knowledge, this rubrene:DBP laser exhibits the largest magnetically induced change in emission brightness reported in a singlet-fission material system to date.^[14,15]

2. Results and Discussion

To study the utility of singlet-fission materials as magnetic field sensors, we fabricate thin films of rubrene doped with 0.5 vol% DBP, a high-photoluminescence quantum yield (PLQY) emitter dye with a singlet state slightly below that of rubrene.^[16] This material system has already earned attention for efficient near-infrared to visible photon upconversion.^[17–20] In this work, we photoexcite rubrene:DBP, creating a population of spin-singlet excitons in the film (**Figure 1a**). These singlets either transfer to the lower-energy singlet state of DBP via Förster resonance energy transfer (FRET) or undergo singlet fission to create two lower-energy spin-triplet excitons. Some of these triplets decay nonradiatively, while others undergo TTA back to the singlet. The majority of singlets in rubrene ultimately transfer to the lower-energy singlet state of DBP before emitting light, resulting in a red-shift between sample absorption and emission (**Figure 1b**).

The presence of a magnetic field changes the number of triplet–triplet pair states with partial spin-singlet character and consequently affects the singlet-fission rate. The number of triplet–triplet pairs with partial singlet character increases to six under weak magnetic fields and decreases to two under strong fields.^[12,21] Therefore, under sufficiently high magnetic field, a decrease in the effective singlet-fission rate is observed in accordance with Merrifield Theory, resulting in an increase in the population of singlets relative to triplets.^[13,22] Because the decay of singlets to the ground state is a classically spin-allowed transition, the observed effect is an increase in brightness of the film as a function of applied magnetic field, as shown for a 100 nm film of rubrene:DBP (0.5 vol%) in **Figure 1c**. The brightness increases substantially above 30 mT, reaching $\approx 8\%$ at 0.4 T applied field, beyond which minimal additional enhancement in photoluminescence is observed. This modulation is lower than the $\approx 22\%$ increase in brightness that we measured in thermally evaporated neat rubrene films, likely due to the reduced coupling strength between rubrene molecules when DBP is doped into the film (see **Figure S1** in the Supporting Information). While doping 0.5 vol% DBP into rubrene reduces the magnetic field effect measured in our rubrene:DBP films, it increases their PLQY from $(3.5 \pm 0.2)\%$ to $(43 \pm 2)\%$. The substantial improvement in PLQY upon doping with DBP suggests that energy transfer to DBP kinetically outcompetes the ≈ 110 ps fission process.^[23]

In our measurements of magnetic field effect, detected photons can result either from prompt emission from the singlet state or from delayed singlet emission following TTA from triplet pair states. Because prompt emission has no magnetic field dependence, restricting detection to delayed fluorescence should increase the magnetic sensitivity of the measurement. Indeed, we find from transient photoluminescence measurements that excluding the first 5 ns of rubrene emission during our analysis enhances the measured 0.4 T magnetic field response in neat rubrene from $\approx 22\%$ to $\approx 40\%$ (**Figure S1**, Supporting Information), consistent with earlier reports of magnetic field effects on delayed emission in amorphous rubrene.^[24] The transient photoluminescence data for rubrene indicate increased magnetic field effects at moderate time scales following prompt singlet emission. The magnetic field effect then decreases after ≈ 50 ns and approaches zero by ≈ 80 ns. This decline in magnetic field effect up to and beyond ≈ 80 ns is likely due to gradual spin decoherence of the initially spin-correlated triplet pair states generated by singlet fission, resulting in nongeminate triplet recombination outweighing geminate triplet recombination at later times.^[25,26]

The modulation in brightness of singlet-fission materials under applied magnetic field make them remarkably effective for magnetic field sensing. To probe the ability of rubrene to resolve spatial differences in magnetic field, we place a 1 in. \times 1 in. film of thermally evaporated rubrene atop two cylindrical 0.4 T permanent magnets (**Figure 2a**). We excite the full area of the film using a blue LED (420 nm, ≈ 2 mW cm^{−2}), while detecting emission through a 550 nm colored glass longpass filter on an iPhone 6S camera, with and without the presence of the magnets. A third-party application called Yamera is used to manually fix iPhone camera aperture and exposure times so that image intensities can be directly compared (see **Figure S2** in

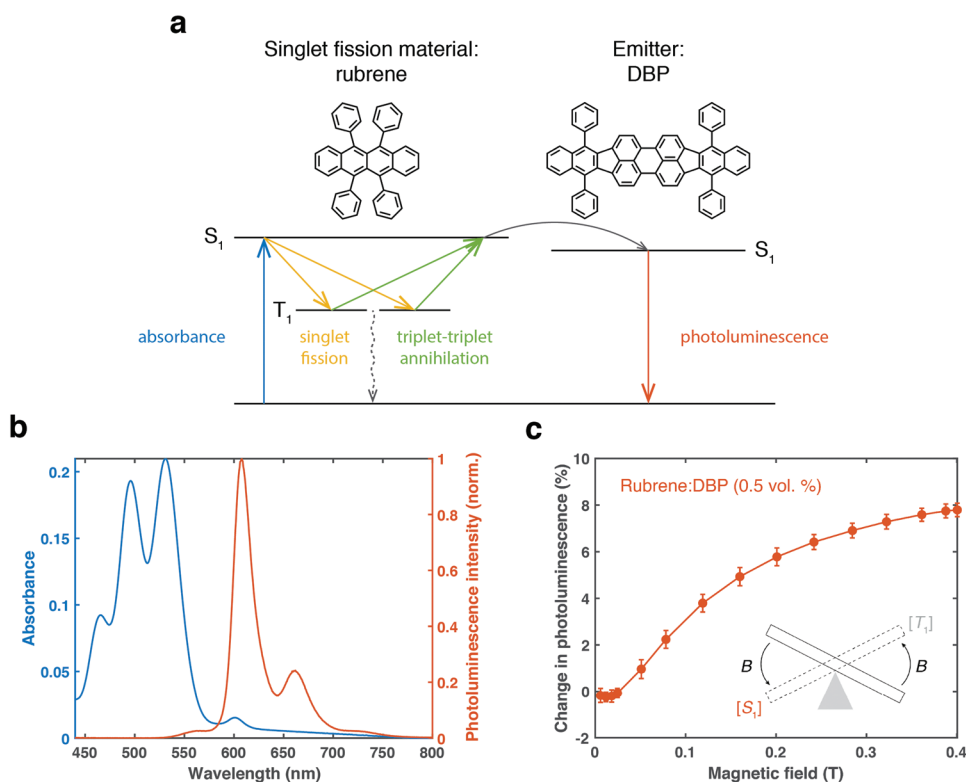


Figure 1. a) Energy state diagram and molecular structures of rubrene:DBP system. Optical pumping creates a population of singlet excitons in rubrene ($S_1 = 2.2$ eV), some of which undergo singlet-exciton fission to create triplet-triplet pairs ($T_1 = 1.14$ eV), which may then recombine to form a singlet exciton or decay to the ground state. An emitter molecule, DBP ($S_1 = 2.0$ eV), is doped into the rubrene film at 0.5% by volume to capture singlet excitons from rubrene and increase the photoluminescence quantum yield of the film.^[16,18] b) Absorbance and emission spectra of a film of rubrene:DBP (0.5 vol%). c) Magnetic field effect on the photoluminescence of a film of rubrene:DBP (0.5 vol%), reported as the percent change in singlet-exciton photoluminescence intensity as a function of applied magnetic field. Error bars represent the standard deviation of nine data points. As illustrated by the seesaw, application of a magnetic field ($B > 0.03$ T) increases the singlet-exciton density, $[S_1]$, and decreases the triplet exciton density, $[T_1]$, resulting in an increase in photoluminescence.

the Supporting Information for a photograph of the complete apparatus).

Figure 2b shows the fractional increase in brightness of the rubrene film, together with contour lines showing the spatial variation of the magnetic field modulation. Dotted white lines indicate the position of the cylindrical magnets beneath the film. For comparison, Figure 2c shows the theoretical spatial magnetic field effect for a thin film of rubrene with this magnet configuration, accounting for substrate thickness. The image intensity across 1×1500 pixels at the center of the camera is plotted in Figure 2d, along with rubrene's expected magnetic field effect. The experimental data show strong qualitative and quantitative agreement with theory and produce a mapping of the magnetic field with ≈ 0.3 mm spatial resolution and ability to sense magnetic fields as low as ≈ 5 mT. Accurate magnetic field mapping is possible above ≈ 30 mT, while below 30 mT, ambiguity is introduced, since multiple field strengths result in the same output modulation. The spatial resolution and magnetic sensitivity of this technique is limited by camera resolution. We expect that by combining a state-of-the-art camera with image analysis software to avoid discontinuities in the imaged magnetic field, the technique could map magnetic field strengths above ≈ 1 mT with a spatial resolution limited by the method of optical interrogation.

To demonstrate the utility of singlet-fission materials as strong magneto-optical modulators for imaging applications, we herein present the fabrication and characterization of a magnetic-field-switchable laser, which exploits the magnetic field dependence of singlet fission to modulate device operation below and above lasing threshold with an external magnetic field. Our device design is based on methods for fabrication of optically-pumped organic semiconductor waveguide lasers developed in the late 1990s.^[27,28] We prepare a rubrene:DBP slab waveguide laser by thermally coevaporating 100 nm of rubrene doped with 0.5 vol% DBP atop a silicon wafer buffered by 2 μm of thermal SiO_2 , cleaved to create two parallel facets (see inset of Figure 3a). The mismatch in the index of refraction between rubrene:DBP and air causes roughly 7% reflection at each interface. When optically pumped with a pulsed nitrogen laser focused to a narrow stripe, the system acts as a crude waveguide laser, with emission guided to the device edges within the high-refractive-index rubrene:DBP layer. The 2 μm silica buffer minimizes parasitic absorption of the lasing modes by the underlying silicon substrate (Figure S4, Supporting Information).

Low-resolution edge emission from a rubrene:DBP slab waveguide laser is shown in Figure 3a, showing clear evidence of spectral narrowing with increasing pump power.

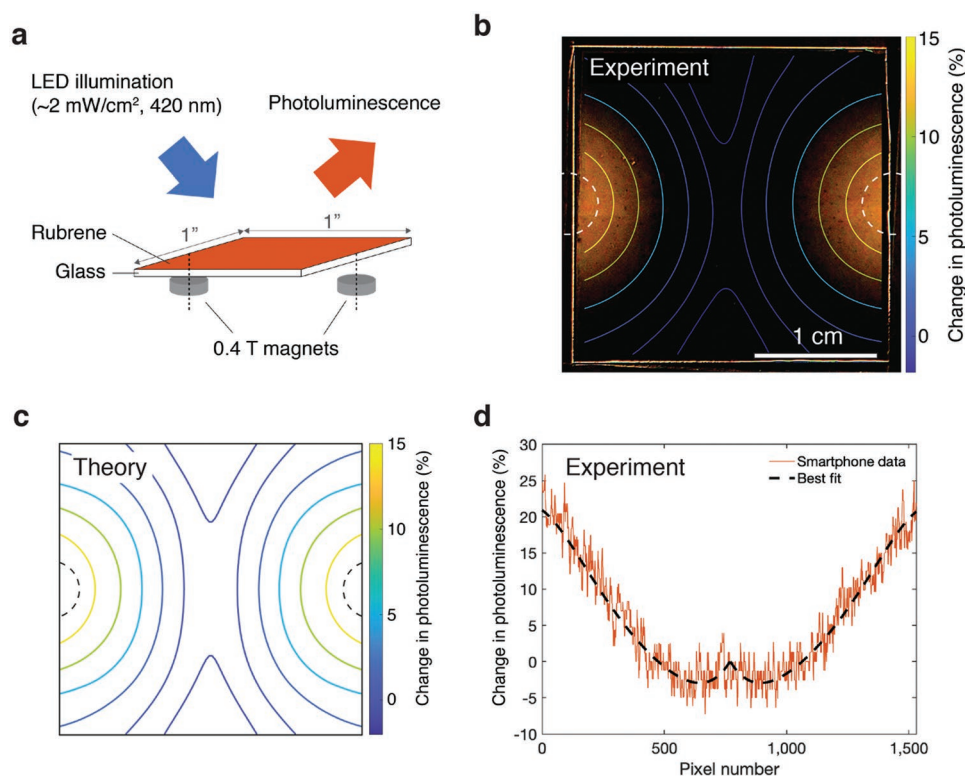


Figure 2. a) Schematic of experimental setup. b) Experimentally measured magnetic field effect in a 1 in. \times 1 in. film of thermally evaporated rubrene resulting from two cylindrical magnets positioned as indicated by the dashed lines, measured using photographs from an iPhone 6S camera with custom control of aperture and exposure time, reported as a fractional change in photoluminescence intensity relative to the photoluminescence at zero magnetic field. Small black spots are a result of degradation in the rubrene film. c) Contour map of modeled magnetic field effect in a 1 in. \times 1 in. film of rubrene resulting from two cylindrical magnets positioned as indicated by the dashed lines. d) Intensity across a 1-pixel-tall horizontal line along the middle of the image from subfigure (b), along with the best fit of the magnetic field effect in rubrene from Figure S1 (Supporting Information).

The emission peak at 663 nm is red-shifted from the DBP emission peak of 612 nm due to absorption by DBP along the length of the waveguide (Figure S3, Supporting Information). High-resolution edge emission reveals multimode lasing, with sharp, narrowly-spaced emission peaks (Figure 3b). The number of lasing modes observed depends highly on excitation position, likely due to imperfections in the waveguide facets caused during silicon wafer cleaving (Figure S5, Supporting Information). Figure 3c shows spatial narrowing of the edge emission with increasing laser power. The spatial narrowing when operating near and above the lasing threshold is consistent with gain-guiding observed in other organic slab waveguide lasers, where the optical mode is confined to regions where the optical gain is maximized.^[28] Above the lasing threshold, the laser emission can be imaged on a beam card (Figure 3d).

To probe the magnetic field dependence of lasing in the rubrene:DBP slab waveguide, we modulate the pump power and magnetic field simultaneously with the apparatus depicted in Figure 4a. To avoid changing the number of lasing modes (which would in turn affect the lasing threshold), we maintain a constant sample position, with pump power controlled using a variable neutral density filter attached to an automated 1D translation stage. Input pulse energy is measured using a

portion of the incident beam diverted with a 90:10 beamsplitter, while output pulse energy is detected on a thermoelectrically cooled silicon camera.

Figure 4b shows the magnetic field dependence of the laser response, demonstrating switching between sub-threshold and above-threshold operation and a +360% enhancement in output intensity at an input pump energy of ≈ 2.4 nJ. Error bars represent the standard deviation of ten data points, due to noise in the collected emission and pulse-to-pulse variation in excitation power. The inset shows how the edge emission spectrum changes with applied magnetic field for the highlighted data points. Fitting the rightmost four data points of each curve, we estimate the lasing threshold of the device to be 2.49 nJ at zero applied magnetic field and 2.31 nJ at 0.4 T applied magnetic field, representing an $\approx 7.2\%$ decrease in lasing threshold with applied field. These results are in good agreement with theory based on the $\approx 8\%$ modulation in steady-state rubrene:DBP photoluminescence from Figure 1c. (See the Supporting Information for a derivation of the expected change in lasing threshold with magnetic field.) Finally, we demonstrate that our rubrene:DBP laser can be repeatedly modulated between “off” and “on” states with an external magnetic field (Figure 4c), with a speed of switching of 0.2 s, as limited by the response time of the electromagnet.

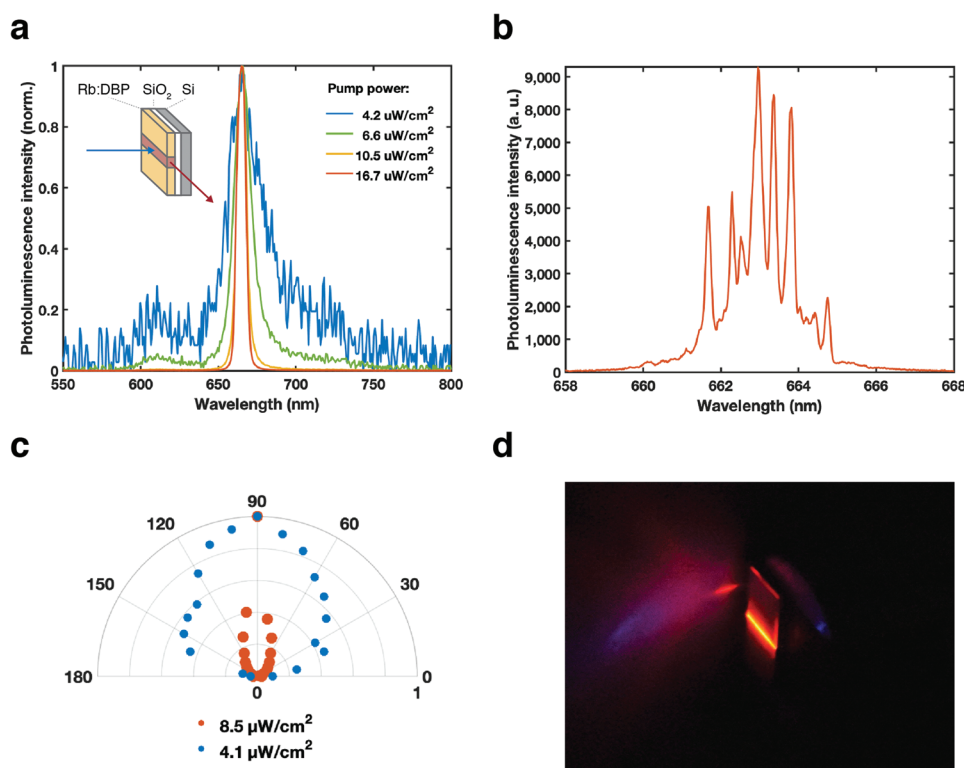


Figure 3. a) Narrowing of photoluminescence spectra from rubrene:DBP edge emission as a function of average pump power. The inset shows the device structure. b) Multimode lasing from a rubrene:DBP device, as measured from a high-resolution edge emission spectrum on a Princeton Instrument PIXIS100 silicon camera with an 1800 g mm^{-1} grating. c) Emission anisotropy from a rubrene:DBP device. Above the lasing threshold, a significant narrowing in the emission profile is observed. d) Photograph of a rubrene:DBP slab waveguide laser, showing emission from one of the device facets imaged on a beam card.

3. Conclusions

Materials with large magneto-optical interactions are interesting for their potential use as magnetic field sensors in spintronics, magnetic resonance imaging, and radiology. Singlet-exciton fission materials are a promising low-cost substitute for conventional magneto-optical materials, as they can exhibit strong optomagnetic interactions and their brightness can be modulated by magnetic field. In this study, we have demonstrated the utility of singlet-fission materials as magnetic field sensors by generating a spatial mapping of the magnitude of a magnetic field across a film of rubrene. Restricting detection to delayed fluorescence enhances the magnetic field effect in rubrene from 22% to 40%, providing improved sensitivity. Finally, we show +360% magnetic field modulation in a first-of-its-kind magnetic-field-switchable singlet-fission laser. Both delayed fluorescence and laser emission can be used to discriminate the magneto-optical signal from background light.

Singlet-fission materials do not presently compete with state-of-the-art magnetic sensors in terms of absolute magnetic sensitivity, but their low cost and biocompatibility make them promising candidates for biological magnetic sensing applications. While rubrene is susceptible to quenching by oxygen's 0.98 eV singlet state,^[29] it is a relatively stable dye.^[30] Stability could be enhanced by using other photostable singlet-fission materials such as perylene diimides, or through micellar or

nanoparticle encapsulation.^[31,32] Nanoparticle encapsulation of singlet-fission materials could have the added potential benefit of exploiting whispering gallery modes to form an optical cavity in the nanoparticle.^[33]

The utility of singlet-fission materials as magnetic field sensors depends both on their absolute response to magnetic field, as well as on their ability to resolve spatial magnetic field variations. While we have shown that neat rubrene allows for low-cost spatial magnetic field imaging, its sensitivity is limited by the modest +22% modulation in fluorescence. Further improvement in sensitivity may be achievable by using singlet-fission films with stronger magnetic field effects. For example, replacing the rubrene film with a film of anthracene crystals sensitized by Rhodamine B could exhibit modulations in delayed emission of up to +60% at magnetic fields as low as ≈ 0.01 T.^[15] We have demonstrated that spectral narrowing and magnetic modulation of at least +360% is possible via magnetically switched lasing in rubrene:DBP, though here, the slab waveguide geometry of the lasers restricts their usefulness for large-area imaging applications. Achieving both high magnetic field sensitivity and spatial resolution may be realizable by borrowing the geometry of vertical-cavity surface-emitting lasers (VCSELs). VCSELs typically consist of a gain medium deposited between two distributed Bragg reflector (DBR) mirrors, or one DBR mirror and a highly reflective material such as silver.^[34] Previous demonstrations have shown that organic materials

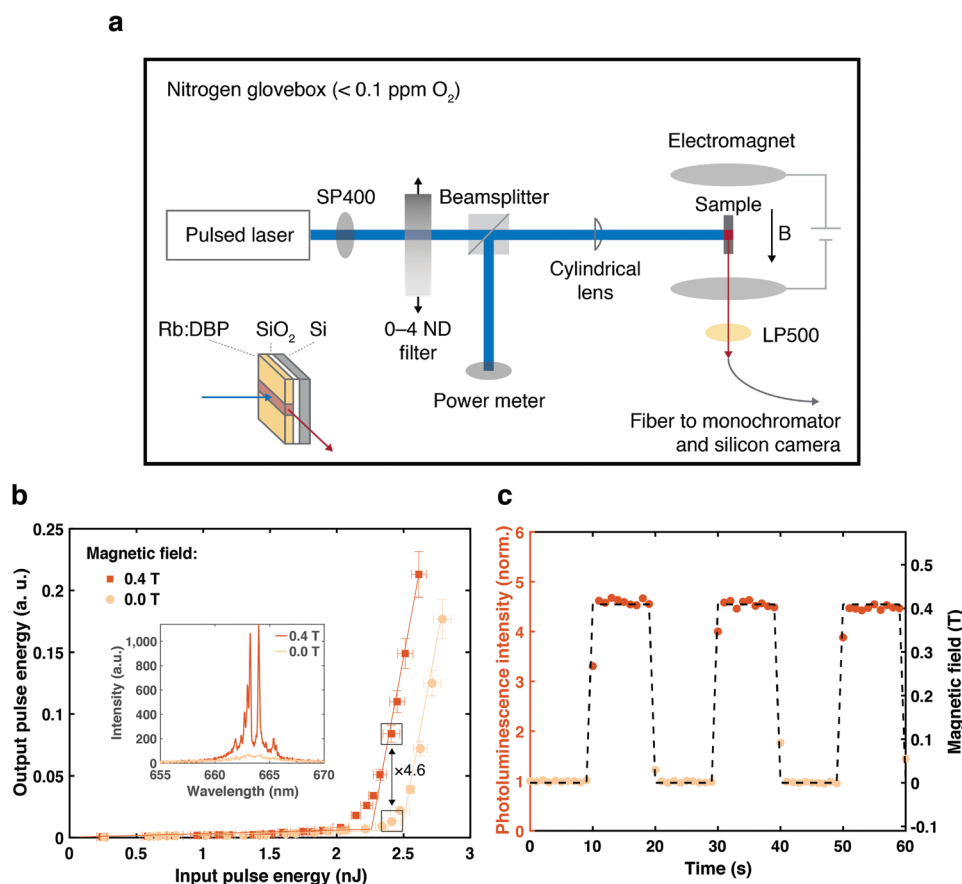


Figure 4. a) Experimental apparatus for measuring the effect of magnetic field on optically pumped emission from a Si/SiO₂/Rb:DBP (0.5 vol%) device. b) Dependence of the Rb:DBP output energy on input pump energy near threshold, as a function of magnetic field. The error bars represent the standard deviation of ten data points. Inset: Edge emission spectra of Rb:DBP device operated with a set input pulse energy near the lasing threshold, with and without applied magnetic field. c) Integrated emission intensity from 655 to 670 nm at edge of Rb:DBP device with and without an applied magnetic field, operated with a set input pulse energy near the lasing threshold. Switching is achieved within 0.2 s, as limited by the response time of the electromagnet.

used in slab waveguide lasers can be incorporated in VCSELs to create surface-emitting lasers with dimensions limited by the deposition technique.^[35]

In conclusion, singlet fission provides a tunable approach to magnetic field sensing, allowing for modulation of dyes between dark and bright states, which can be readily characterized by delayed fluorescence and laser emission. Based on the proposed mechanisms that allow birds to sense Earth's magnetic fields above $\approx 20 \mu\text{T}$,^[36] additional gains in magnetic sensitivity may be realizable by designing molecular systems for triplet-charge rather than triplet-triplet interactions.^[37] Further studies could focus on increasing the magneto-optical modulation from spin-triplet interactions, demonstrating volumetric magnetic field imaging, and encapsulating singlet-fission materials for targeted bioimaging and bioassays.

4. Experimental Section

Sample Preparation: Details of the sample preparation are included in the Supporting Information.

Sample Characterization: Details of the measurements are included in the Supporting Information.

Supporting Information

Supporting Information is available from the Wiley Online Library or from the author.

Acknowledgements

C.F.P., M.E., and J.F. were supported by the U.S. Department of Energy, Office of Basic Energy Sciences, Division of Materials Sciences and Engineering (Award No. DE-FG02-07ER46454). C.F.P. also acknowledges a National Science Foundation Graduate Research Fellowship under Grant No. 1122374.

Conflict of Interest

The authors declare no conflict of interest.

Author Contributions

C.F.P. contributed to project development, device fabrication, spectroscopy, measurement automation, analysis, and writing, M.E. assisted with measurement automation, and J.F. assisted with spatial imaging.

Data Availability Statement

The data that support the findings of this study are available from the corresponding author upon reasonable request.

Keywords

lasers, magnetic field imaging, magnetic sensors, optical modulators, singlet fission, triplet-triplet annihilation, upconversion

Received: May 22, 2021

Revised: September 23, 2021

Published online: December 4, 2021

- [1] P. P. Freitas, F. A. Cardoso, V. C. Martins, S. A. M. Martins, J. Loureiro, J. Amaral, R. C. Chaves, S. Cardoso, L. P. Fonseca, A. M. Sebastião, M. Pannetier-Lecoeur, C. Fermon, *Lab Chip* **2011**, 12, 546.
- [2] S. Xu, V. V. Yashchuk, M. H. Donaldson, S. M. Rochester, D. Budker, A. Pines, *Proc. Natl. Acad. Sci. USA* **2006**, 103, 12668.
- [3] A. Soheilian, M. Ranjbaran, M. M. Tehrani, *Sci. Rep.* **2020**, 10, 1294.
- [4] S. Kumari, S. Chakraborty, *J. Sens. Sens. Syst.* **2018**, 7, 421.
- [5] A. Boretti, L. Rosa, J. Blackledge, S. Castelletto, *Beilstein J. Nanotechnol.* **2019**, 10, 2128.
- [6] C. Foy, C. Foy, L. Zhang, M. E. Trusheim, M. E. Trusheim, K. R. Bagnall, M. Walsh, M. Walsh, E. N. Wang, D. R. Englund, D. R. Englund, *ACS Appl. Mater. Interfaces* **2020**, 12, 26525.
- [7] L. Gloag, M. Mehdipour, D. Chen, R. D. Tilley, J. J. Gooding, *Adv. Mater.* **2019**, 31, 1904385.
- [8] M. Schubert, L. Woolfson, I. R. M. Barnard, A. M. Dorward, B. Casement, A. Morton, G. B. Robertson, P. L. Appleton, G. B. Miles, C. S. Tucker, S. J. Pitt, M. C. Gather, *Nat. Photonics* **2020**, 14, 452.
- [9] A. Pinzon-Rodriguez, S. Bensch, R. Muheim, *J. R. Soc. Interface* **2018**, 15, 20180058.
- [10] A. Günther, A. Einwich, E. Sjulstok, R. Feederle, P. Bolte, K. W. Koch, I. A. Solov'yov, H. Mouritsen, *Curr. Biol.* **2018**, 28, 211.
- [11] M. D. Lumb, L. Spectroscopy, *Luminescence Spectroscopy*, Academic Press, London, UK **1978**.
- [12] R. C. Johnson, R. E. Merrifield, *Phys. Rev. B* **1970**, 1, 896.
- [13] R. E. Merrifield, *J. Chem. Phys.* **1968**, 48, 4318.
- [14] M. B. Smith, J. Michl, *Chem. Rev.* **2010**, 110, 6891.
- [15] R. P. Groff, R. E. Merrifield, A. Suna, P. Avakian, *Phys. Rev. Lett.* **1972**, 29, 429.
- [16] J. D. Debad, J. C. Morris, V. Lynch, P. Magnus, A. J. Bard, *J. Am. Chem. Soc.* **1996**, 118, 2374.
- [17] S. Wieghold, A. S. Bieber, Z. A. VanOrman, L. Daley, M. Leger, J. P. Correa-Baena, L. Nienhaus, *Matter* **2019**, 1, 705.
- [18] M. Wu, D. N. Congreve, M. W. B. Wilson, J. Jean, N. Geva, M. Welborn, T. Van Voorhis, V. Bulovic, M. G. Bawendi, M. A. Baldo, *Nat. Photonics* **2016**, 10, 31.
- [19] L. Nienhaus, M. Wu, N. Geva, J. J. Shepherd, M. W. B. Wilson, V. Bulović, T. Van Voorhis, M. A. Baldo, M. G. Bawendi, *ACS Nano* **2017**, 11, 7848.
- [20] M. Wu, J. Jean, V. Bulović, M. A. Baldo, *Appl. Phys. Lett.* **2017**, 110, 211101.
- [21] V. Ern, R. E. Merrifield, *Phys. Rev. Lett.* **1968**, 21, 609.
- [22] T. C. Wu, N. J. Thompson, D. N. Congreve, E. Hontz, S. R. Yost, T. Van Voorhis, M. A. Baldo, *Appl. Phys. Lett.* **2014**, 104, 193901.
- [23] S. R. Yost, J. Lee, M. W. B. Wilson, T. Wu, D. P. McMahon, R. R. Parkhurst, N. J. Thompson, D. N. Congreve, A. Rao, K. Johnson, M. Y. Sfeir, M. G. Bawendi, T. M. Swager, R. H. Friend, M. A. Baldo, T. Van Voorhis, *Nat. Chem.* **2014**, 6, 492.
- [24] G. B. Piland, J. J. Burdett, D. Kurunthu, C. J. Bardeen, *J. Phys. Chem. C* **2013**, 117, 1224.
- [25] H. L. Stern, A. Cheminal, S. R. Yost, K. Broch, S. L. Bayliss, K. Chen, M. Tabachnyk, K. Thorley, N. Greenham, J. M. Hodgkiss, J. Anthony, M. Head-Gordon, A. J. Musser, A. Rao, R. H. Friend, *Nat. Chem.* **2017**, 9, 1205.
- [26] E. A. Wolf, D. M. Finton, V. Zoutenbier, I. Biaggio, *Appl. Phys. Lett.* **2018**, 112, 083301.
- [27] V. G. Kozlov, S. R. Forrest, *Curr. Opin. Solid State Mater. Sci.* **1999**, 4, 203.
- [28] P. E. Burrows, S. R. Forrest, V. G. Kozlov, V. Bulovic, *Nature* **1997**, 389, 362.
- [29] S. Feng, M. Huang, J. R. Lamb, W. Zhang, R. Tatara, Y. Zhang, Y. Guang Zhu, C. F. Perkinson, J. A. Johnson, Y. Shao-Horn, *Chem* **2019**, 5, 2630.
- [30] T. Hasegawa, J. Takeya, *Sci. Technol. Adv. Mater.* **2009**, 10, 024314.
- [31] S. N. Sanders, M. K. Gangishetty, M. Y. Sfeir, D. N. Congreve, *J. Am. Chem. Soc.* **2019**, 141, 9180.
- [32] H. Kouno, Y. Sasaki, N. Yanai, N. Kimizuka, *Chem. - Eur. J.* **2019**, 25, 6124.
- [33] P. T. Snee, Y. Chan, D. G. Nocera, M. G. Bawendi, *Adv. Mater.* **2005**, 17, 1131.
- [34] R. Michalzik, *VCSELs: Fundamentals, Technology and Applications of Vertical-Cavity Surface-Emitting Lasers*, Springer, Berlin, Germany **2013**.
- [35] V. G. Kozlov, V. Bulovic, P. E. Burrows, M. Baldo, V. B. Khalfin, G. Parthasarathy, S. R. Forrest, Y. You, M. E. Thompson, *J. Appl. Phys.* **1998**, 84, 4096.
- [36] K. Schulten, C. E. Swenberg, A. Weller, *Z. Phys. Chem.* **1978**, 111, 1.
- [37] P. J. Hore, H. Mouritsen, *Annu. Rev. Biophys.* **2016**, 45, 299.